

State estimation in range coordinate using range-only measurements

LI Keyi, GUO Zhengkun, and ZHOU Gongjian*

School of Electronics and Information Engineering, Harbin Institute of Technology, Harbin 150001, China

Abstract: In some tracking applications, due to the sensor characteristic, only range measurements are available. If this is the case, due to the lack of full position measurements, the observability of Cartesian states (e.g., position and velocity) are limited to particular cases. For general cases, the range measurements can be utilized by developing a state estimation algorithm in range-Doppler (R-D) plane to obtain accurate range and Doppler estimates. In this paper, a state estimation method based on the proper dynamic model in the R-D plane is proposed. The unscented Kalman filter is employed to handle the strong nonlinearity in the dynamic model. Two filtering initialization methods are derived to extract the initial state estimate and the initial covariance in the R-D plane from the first several range measurements. One is derived based on the well-known two-point differencing method. The other incorporates the correct dynamic model information and uses the unscented transformation method to obtain the initial state estimates and covariance, resulting in a model-based method, which capitalizes the model information to yield better performance. Monte Carlo simulation results are provided to illustrate the effectiveness and superior performance of the proposed state estimation and filter initialization methods.

Keywords: range-only measurement, state estimation, filter initialization, target tracking, unscented Kalman filter (UKF).

DOI: 10.23919/JSEE.2022.000050

1. Introduction

In many tracking applications, the states of a target (e.g., position and velocity) are estimated from full position measurements, which are usually reported in polar or spherical coordinates. However, in some practical applications, due to the sensor characteristics, only range and/or Doppler measurements are available or reliable in the tracking process. For example, in inverse synthetic aperture radar (ISAR), the output of the range-only or range-Doppler-only tracker is utilized to control the range gate

and antenna pointing for extended data collection [1]. In high frequency surface wave radar (HFSWR), when tracking algorithms using only range and/or Doppler measurements are applied, efforts and expenses for building a large and expensive antenna array, which is used to obtain a narrow beam due to the large wavelength at high frequency (HF), can be saved [2]. In addition, some passive radars, such as Lockheed Martin's Silent Sentry system, work at low frequencies, which makes them difficult to provide accurate azimuth measurements for target tracking [3].

In recent years, target tracking with only range and/or Doppler measurements has attracted increasing attention. For the cases with a single sensor, the observability of target tracking with range-only measurements is investigated in [4–7] and it is concluded that some known maneuvers are required to guarantee the observability of Cartesian states. A Gaussian mixture filter was presented in [8] to eliminate inaccurate estimates for range-only tracking. For the cases with multiple sensors, combining the data offers the opportunity to locate targets using the trilateration method [9]. In [2,10–18], target tracking or localization with only range and/or Doppler measurements provided by multi-static or multi-monostatic sensors was explored. This can be considered as a crucial technology of the future for the application of low-cost sensor networks to replace large aperture antennas [19,20]. A proof-of-concept of target tracking in range coordinate using range-only measurements, which is beneficial to alleviate multi-sensor data association burden by eliminating clutter in the single sensor stage, was presented in [10]. However, the targets are assumed to move with constant accelerations in range coordinates, performance may be degraded due to the usage of inaccurate motion models.

To find more accurate motion models, the authors of [21,22] take efforts to the motion modeling in the range coordinates. An effective state estimation method using range and Doppler measurements is proposed to produce state estimates in the range-Doppler (R-D) plane.

Manuscript received March 06, 2021.

*Corresponding author.

This work was supported by the National Natural Science Foundation of China (61671181; 62101162).

In some practical applications, due to the characteristics of the sensor system or the effect of Doppler ambiguity, only the range measurements are available or reliable. The motion models in [21,22] also offer the opportunity to extract more accurate range estimates from range-only measurements. The enhancement of range estimation benefits the tracking performance based on multisensor data fusion using the trilateration method [9], which does not require angle or Doppler information to locate the target. That is, the efforts on building a large and expensive antenna array to obtain accurate angle measurements and solving the Doppler ambiguity to obtain accurate Doppler measurements can be saved. Therefore, a state estimation method that effectively utilizes the accurate R-D motion models and range-only measurements to obtain accurate range estimates is desired, which motivates this paper.

In this paper, the state estimation problem in range coordinates using range-only measurements is investigated and a state estimation method is proposed. The motion model in the R-D plane for the Cartesian motion in [21] is adopted to formulate the state equation in the proposed method. To handle the nonlinearity of the dynamic model, the unscented Kalman filter (UKF) [23–27] is adopted to process range measurements. For the initialization of the state vector in the R-D plane using range-only measurements, two filter initialization methods are proposed. One is derived in an analytical form based on the well-known two-point differencing (TPD) approach, which holds the assumption that the target range changes linearly with time. However, it is not usually the case, as stated in [21]. Therefore, this paper may suffer from performance degradation when the assumption is violated. To overcome this problem, a new model-based (MB) filter initialization method, which incorporates the correct information of the dynamic model into the initialization process, is developed in this paper. By solving a series of equations constructed based on the dynamic model, a nonlinear function of the state with respect to the range component is derived. Since the initial estimate of Doppler cannot be expressed in an analytical form using range-only measurements, the initial state estimate and the covariance matrix are calculated using the unscented transformation (UT) method [23–24] according to the nonlinear function. In numerical experiments, the proposed state estimation methods using the two initialization methods are compared against existing state estimation methods using approximate models. The posterior Cramer-Rao lower bound (PCRLB) is calculated as a theoretical performance benchmark. The comparison results demonstrate the effective and superior performance of the proposed approach of state estimation and filter initializa-

tion using range-only measurement.

This paper is a refined and expanded version of a previous conference paper [28]. The contributions of this paper are summarized as follows.

(i) The state estimation method using range-only measurements developed based on the accurate motion model in the R-D plane and the UKF is introduced in detail.

(ii) Two filter initialization methods are presented. Besides the TPD-based method, an MB filter initialization method is proposed. The derivation of the initial state estimate and the calculation of the initial covariance are given.

(iii) Various illustrative examples in different conditions are included to demonstrate the effectiveness of the proposed method along with more in-depth discussions about the performance.

This paper is organized as follows. The state estimation problem using range-only measurements is formulated in Section 2. In Section 3, the filtering procedure is presented. Two corresponding filter initialization methods are deduced in Section 4. In Section 5, Monte Carlo simulations are provided. Finally, conclusions are given in Section 6.

2. Problem statement

In Cartesian coordinates, the nearly constant velocity (NCV) motion, which assumes that the target moves with a nearly constant velocity, can be modeled as

$$\begin{cases} x_{k+1} = x_k + \dot{x}_k T + \frac{T^2}{2} v_k^x \\ \dot{x}_{k+1} = \dot{x}_k + T v_k^x \\ y_{k+1} = y_k + \dot{y}_k T + \frac{T^2}{2} v_k^y \\ \dot{y}_{k+1} = \dot{y}_k + T v_k^y \end{cases} \quad (1)$$

where x_k and y_k are position components along x and y axes respectively at time step k , \dot{x}_k and \dot{y}_k are corresponding velocity components, v_k^x and v_k^y are mutually independent zero-mean Gaussian white noises along x and y directions with standard deviation q , and T stands for the sampling interval. This model is a commonly used non-maneuvering model.

In range coordinates, the motion model corresponding to the NCV model in Cartesian coordinates has been presented in [14], where the state vector is defined as

$$\mathbf{x}_k = \begin{bmatrix} r_k \\ \dot{r}_k \\ \dot{\eta}_k \end{bmatrix} = \begin{bmatrix} \sqrt{x_k^2 + y_k^2} \\ x_k \dot{x}_k + y_k \dot{y}_k \\ \sqrt{\dot{x}_k^2 + \dot{y}_k^2} \end{bmatrix} \quad (2)$$

where r_k is the range component, \dot{r}_k is the Doppler component, $\dot{\eta}_k$ is the component of the first-order derivative

of the converted Doppler component η_k that equals the product of range and Doppler components $r_k \cdot \dot{r}_k$ [29,30].

Substitute the evolutions of Cartesian states in (1) into the state vector in range coordinate at time step $k+1$, the range component can be written as

$$r_{k+1} = \sqrt{(r_{k+1}^s)^2 + \Delta h} \quad (3)$$

where

$$r_{k+1}^s = \sqrt{r_k^2 + 2r_k \dot{r}_k T + \dot{\eta}_k T^2},$$

$$\Delta h = \frac{T^4}{4}(v_k^x)^2 + \frac{T^4}{4}(v_k^y)^2 + (x_k + \dot{x}_k T)T^2 v_k^x + (y_k + \dot{y}_k T)T^2 v_k^y.$$

A Taylor expansion is applied to simplify the motion model, resulting in the evolution equation of range as

$$r_{k+1} = r_{k+1}^s + \frac{\Delta h}{2r_{k+1}^s} + O(\Delta h^2) \approx r_{k+1}^s + \tilde{r}_k \quad (4)$$

where

$$\tilde{r}_k = \frac{T^4}{8r_{k+1}^s}(v_k^x)^2 + \frac{T^4}{8r_{k+1}^s}(v_k^y)^2 + \frac{(x_k + \dot{x}_k T)T^2}{2r_{k+1}^s}v_k^x + \frac{(y_k + \dot{y}_k T)T^2}{2r_{k+1}^s}v_k^y$$

is the random part, i.e., the process noise.

The evolution equations of \dot{r}_{k+1} and $\dot{\eta}_{k+1}$ can be obtained in the same way as

$$\dot{r}_{k+1} = \frac{r_k \dot{r}_k + \dot{\eta}_k T}{r_{k+1}^s} + \tilde{r}_k, \quad (5)$$

$$\dot{\eta}_{k+1} = \dot{\eta}_k + \tilde{\eta}_k. \quad (6)$$

Note that the means of the process noise are not necessarily to be zero. To ensure the process noises are zero-mean, the non-zero means are eliminated from the process noise vector, resulting in the state equation as

$$\mathbf{x}_{k+1} = \begin{bmatrix} r_{k+1} \\ \dot{r}_{k+1} \\ \dot{\eta}_{k+1} \end{bmatrix} = f(\mathbf{x}_k) + u(\mathbf{x}_k) + \mathbf{v}_k = \begin{bmatrix} r_{k+1}^s \\ r_k \dot{r}_k + \dot{\eta}_k T \\ r_{k+1}^s \\ \dot{\eta}_k \end{bmatrix} + \begin{bmatrix} \frac{q^2 T^4}{4r_{k+1}^s} \\ \frac{q^2 T^3}{r_{k+1}^s} \\ 2q^2 T^2 \end{bmatrix} + \mathbf{v}_k \quad (7)$$

where $f(\cdot)$ is the nonlinear transition function, $u(\cdot)$ is the function containing means of the process noise, denotes the deterministic part of range evolved from \mathbf{x}_k , and \mathbf{v}_k is the process noise vector with covariance \mathbf{Q}_k given by

$$\mathbf{Q}_k = \begin{bmatrix} \sigma_k^{rr} & \sigma_k^{r\dot{r}} & \sigma_k^{r\dot{\eta}} \\ \sigma_k^{\dot{r}r} & \sigma_k^{\dot{r}\dot{r}} & \sigma_k^{\dot{r}\dot{\eta}} \\ \sigma_k^{\dot{\eta}r} & \sigma_k^{\dot{\eta}\dot{r}} & \sigma_k^{\dot{\eta}\dot{\eta}} \end{bmatrix} \quad (8)$$

where

$$\sigma_k^{rr} = \frac{q^2 T^4}{4} + \frac{q^4 T^8}{16(r_{k+1}^s)^2}, \quad (9)$$

$$\sigma_k^{r\dot{r}} = \sigma_k^{\dot{r}r} = \frac{q^2 T^3}{2} + \frac{q^2 T^4}{4(r_{k+1}^s)^2} r_k \dot{r}_k + \frac{q^2 T^5}{4(r_{k+1}^s)^2} \dot{\eta}_k + \frac{q^4 T^7}{4(r_{k+1}^s)^2}, \quad (10)$$

$$\sigma_k^{r\dot{\eta}} = \sigma_k^{\dot{\eta}r} = \frac{q^2 T^3}{r_{k+1}^s} r_k \dot{r}_k + \frac{q^2 T^4}{r_{k+1}^s} \dot{\eta}_k + \frac{q^4 T^6}{2r_{k+1}^s}, \quad (11)$$

$$\sigma_k^{\dot{r}\dot{r}} = q^2 T^2 + \frac{q^2 T^3}{(r_{k+1}^s)^2} r_k \dot{r}_k + \frac{5q^2 T^4}{4(r_{k+1}^s)^2} \dot{\eta}_k + \frac{q^4 T^6}{(r_{k+1}^s)^2}, \quad (12)$$

$$\sigma_k^{\dot{r}\dot{\eta}} = \sigma_k^{\dot{\eta}\dot{r}} = \frac{2q^2 T^2}{r_{k+1}^s} r_k \dot{r}_k + \frac{3q^2 T^3}{r_{k+1}^s} \dot{\eta}_k + \frac{2q^4 T^5}{r_{k+1}^s}, \quad (13)$$

$$\sigma_k^{\dot{\eta}\dot{\eta}} = 4q^2 T^2 \dot{\eta}_k + 4q^4 T^4. \quad (14)$$

For more details of the derivation of the motion model, please refer to [21]. In the filtering procedure, the state estimates at time step k are substituted into the formulations instead of the unknown true states.

In this problem, only range measurements are assumed to be available. The measurement equation is given by

$$z_k = r_k^m = \mathbf{H}_k \mathbf{x}_k + w_k = \begin{bmatrix} 1 & 0 & 0 \end{bmatrix} \begin{bmatrix} r_k \\ \dot{r}_k \\ \dot{\eta}_k \end{bmatrix} + \tilde{r}_k \quad (15)$$

where $z_k = r_k^m$ is the range measurement, \mathbf{H}_k denotes the measurement matrix, $w_k = \tilde{r}_k$ is the zero-mean white Gaussian measurement noise with covariance $R_k = \sigma_r^2$. Note that the measurement equation is linear.

Based on the state equation in (3) and the measurement equation in (11), this paper aims to develop an effective state estimation method to extract range and Doppler estimates from range-only measurements. The potential applications include ISAR, HFSWR and some passive radars which suffer from coarse azimuth resolution and the effect of Doppler ambiguity. Due to the strong nonlinearity contained in the state equation, a nonlinear filtering method is desired. The lack of Doppler measurement also poses a challenge to the initialization of the Doppler and converted Doppler components in the state vector, which has a significant effect on the overall estimation performance.

3. State estimation in R-D plane

3.1 Filtering

Considering the fact that the state equation in (3) is highly nonlinear, a nonlinear filtering method is needed in the

estimation process. Here, the UKF [23–27] is employed to estimate state in the R-D plane from the range-only measurements. Note that other commonly used nonlinear filtering methods, such as the extended Kalman filter (EKF), the cubature Kalman filter (CKF) [31,32] and the particle filter (PF) [33–36] can also be applied. In this paper, the UKF is chosen since it yields better performance than the EKF when the nonlinearity is strong and requires less computation load than the PF. Based on (7) and (15), the filtering procedure of the resulted method at time step $k \geq 3$ is given as follows:

Algorithm 1 One iteration of the filter in range coordinate

Input $\hat{\mathbf{x}}_{k-1|k-1}$, $\mathbf{P}_{k-1|k-1}$, \mathbf{z}_k

Output $\hat{\mathbf{x}}_{k|k}$, $\mathbf{P}_{k|k}$

Step 1 Calculate $2n_x + 1$ sigma points according to the state estimate $\hat{\mathbf{x}}_{k-1|k-1}$ and corresponding weights to approximate the prior distribution:

$$\begin{cases} \xi_{k-1}^0 = \hat{\mathbf{x}}_{k-1|k-1} \\ \xi_{k-1}^i = \hat{\mathbf{x}}_{k-1|k-1} + (\sqrt{(n_x + \lambda)\mathbf{P}_{k-1|k-1}})_i \\ \xi_{k-1}^{i+n_x} = \hat{\mathbf{x}}_{k-1|k-1} - (\sqrt{(n_x + \lambda)\mathbf{P}_{k-1|k-1}})_i \end{cases}, \quad (16)$$

$$\begin{cases} W^0 = \frac{\lambda}{n_x + \lambda} \\ W^i = \frac{1}{2(n_x + \lambda)} \\ W^{i+n_x} = \frac{1}{2(n_x + \lambda)} \end{cases}, \quad (17)$$

where $i = 1, 2, \dots, n_x$, n_x is the dimension of the state vector \mathbf{x}_k , λ is a scaling parameter satisfying $n_x + \lambda \neq 0$, and $(\sqrt{(n_x + \lambda)\mathbf{P}_{k-1|k-1}})_i$ is the i th row or the i th column of the root mean square matrix $\sqrt{(n_x + \lambda)\mathbf{P}_{k-1|k-1}}$.

Step 2 State prediction:

$$\xi_{k|k-1}^i = f(\xi_{k-1}^i) + u(\xi_{k-1}^i), \quad (18)$$

$$\hat{\mathbf{x}}_{k|k-1} = \sum_{i=0}^{2n_x} W^i \xi_{k|k-1}^i, \quad (19)$$

$$\Delta \mathbf{x}_{k|k-1}^i = \xi_{k|k-1}^i - \hat{\mathbf{x}}_{k|k-1}, \quad (20)$$

$$\mathbf{P}_{k|k-1} = \sum_{i=0}^{2n_x} W^i \Delta \mathbf{x}_{k|k-1}^i (\Delta \mathbf{x}_{k|k-1}^i)' + \mathbf{Q}_{k-1}. \quad (21)$$

Step 3 Filter gain:

$$\mathbf{z}_{k|k-1} = \mathbf{H}_k \hat{\mathbf{x}}_{k|k-1}, \quad (22)$$

$$\mathbf{P}_{zz} = \mathbf{R}_k + \mathbf{H}_k \mathbf{P}_{k|k-1} \mathbf{H}_k', \quad (23)$$

$$\mathbf{P}_{xz} = \mathbf{P}_{k|k-1} \mathbf{H}_k', \quad (24)$$

$$\mathbf{K}_k = \mathbf{P}_{xz} (\mathbf{P}_{zz})^{-1}. \quad (25)$$

Step 4 State update:

$$\hat{\mathbf{x}}_{k|k} = \hat{\mathbf{x}}_{k|k-1} + \mathbf{K}_k (\mathbf{z}_k - \hat{\mathbf{z}}_{k|k-1}), \quad (26)$$

$$\mathbf{P}_{k|k} = \mathbf{P}_{k|k-1} - \mathbf{K}_k \mathbf{P}_{zz} (\mathbf{K}_k)'. \quad (27)$$

Generally, the Cartesian state estimates cannot be determined using the R-D state estimate $\hat{\mathbf{x}}_{k|k}$ without angle information. For the cases with multiple sensors, the trilateration method [9] can be employed to fuse the multiple R-D state estimates to obtain the Cartesian state estimates.

3.2 Performance analysis

The PCRLB is a widely used performance measure [37], which gives a lower bound of the error covariance given by

$$\mathbf{P}_{k|k} = \mathbf{E}[(\hat{\mathbf{x}}_{k|k} - \mathbf{x}_k)(\hat{\mathbf{x}}_{k|k} - \mathbf{x}_k)'] \geq \mathbf{J}_k^{-1} \quad (28)$$

where \mathbf{J}_k is the Fisher information matrix (FIM), $\mathbf{E}(x)$ represents the mean of x . For the state estimation problem in the range coordinate using range-only measurements, the FIM [37] can be calculated recursively by

$$\begin{aligned} \mathbf{J}_{k+1} = & \left[\left(\frac{\partial f(\mathbf{x}_k)}{\partial \mathbf{x}_k} + \frac{\partial u(\mathbf{x}_k)}{\partial \mathbf{x}_k} \right) \mathbf{J}_k^{-1} \right. \\ & \left. \left(\frac{\partial f(\mathbf{x}_k)}{\partial \mathbf{x}_k} + \frac{\partial u(\mathbf{x}_k)}{\partial \mathbf{x}_k} \right)^T + \mathbf{Q}_k \right]^{-1} + \mathbf{J}_{k+1}^z \end{aligned} \quad (29)$$

where $\partial f(\mathbf{x}_k)/\partial \mathbf{x}_k$ is the first-order partial derivative of $f(\mathbf{x}_k)$ with respect to \mathbf{x}_k , the FIM is initialized as $\mathbf{J}_3 = \mathbf{P}_{3|3}$. Matrix \mathbf{J}_{k+1}^z represents the measurement contribution to the PCRLB, which is given by

$$\mathbf{J}_{k+1}^z = \mathbf{H}_k^T \mathbf{R}_k^{-1} \mathbf{H}_k. \quad (30)$$

4. Filter initialization

In this section, two filter initialization methods are developed for the proposed state estimation method. One is derived based on the well-known two-point initialization approach. The other is a model-based method, which incorporates the correct model information by using the UT method [23,24] to calculate the initial state estimate and covariance.

4.1 TPD-based initialization

The TPD method is commonly used in filter initialization of practical tracking applications due to its simplicity of implementation. In Cartesian coordinates, the TPD method assumes that the target state evolves following the constant velocity (CV) model, in which the target position changes linearly with time. The position component is initialized directly by using the corresponding position measurement while the velocity component is obtained as the differencing results of position measure-

ments. Here, an effective method is derived based on TPD for the proposed filter in the range coordinate using range-only measurements.

For the dynamic model defined in (7), the initial state estimate is denoted by

$$\hat{\mathbf{x}}_{3|3} = [\hat{r}_{3|3}, \hat{r}_{3|3}, \hat{\eta}_{3|3}]'. \quad (31)$$

The initial covariance is denoted by

$$\mathbf{P}_{3|3} = \begin{bmatrix} P_{3|3}^{rr} & P_{3|3}^{r\dot{r}} & P_{3|3}^{r\dot{\eta}} \\ P_{3|3}^{r\dot{r}} & P_{3|3}^{\dot{r}\dot{r}} & P_{3|3}^{\dot{r}\dot{\eta}} \\ P_{3|3}^{r\dot{\eta}} & P_{3|3}^{\dot{r}\dot{\eta}} & P_{3|3}^{\dot{\eta}\dot{\eta}} \end{bmatrix}. \quad (32)$$

The range component $\hat{r}_{3|3}$ in (31) is initialized directly by using the range measurement at the third time step as

$$\hat{r}_{3|3} = r_3^m. \quad (33)$$

Based on the TPD method, $\hat{r}_{3|3}$ in (31) is initialized by differencing the range measurements at two consecutive steps:

$$\hat{r}_{3|3} = \frac{r_3^m - r_2^m}{T}. \quad (34)$$

The component of converted Doppler $\eta_3 = r_3 \dot{r}_3$ is also assumed to evolve linearly with time in a sampling interval, thus the initial estimate of its first-order derivation can be calculated by differencing the estimates $\hat{\eta}_{3|3}$ and $\hat{\eta}_{2|2}$ as

$$\hat{\eta}_{3|3} = \frac{\hat{\eta}_{3|3} - \hat{\eta}_{2|2}}{T} = \frac{\hat{r}_{3|3} \hat{r}_{3|3} - \hat{r}_{2|2} \hat{r}_{2|2}}{T}. \quad (35)$$

Substitute (33) and (34) into (35), and $\hat{\eta}_{3|3}$ can be written as

$$\hat{\eta}_{3|3} = \frac{(r_3^m)^2 - (r_2^m)^2 - r_3^m r_2^m + r_2^m r_1^m}{T^2}. \quad (36)$$

The initial state estimate can be written as

$$\hat{\mathbf{x}}_{3|3} = \begin{bmatrix} \hat{r}_{3|3} \\ \hat{\dot{r}}_{3|3} \\ \hat{\eta}_{3|3} \end{bmatrix} = \begin{bmatrix} r_3^m \\ \frac{r_3^m - r_2^m}{T} \\ \frac{(r_3^m)^2 - (r_2^m)^2 - r_3^m r_2^m + r_2^m r_1^m}{T^2} \end{bmatrix}. \quad (37)$$

The corresponding initial covariance matrix can be derived based on the formulation of the initial state estimate. First, the range measurement noise \tilde{r}_k is assumed to be zero-mean Gaussian with known variance σ_r^2 , that is

$$\begin{cases} \mathbf{E}[\tilde{r}_k] = 0 \\ R_k^r = \mathbf{E}[\tilde{r}_k \tilde{r}_k] = \sigma_r^2. \\ \mathbf{E}[\tilde{r}_k \tilde{r}_l] = 0, \quad k \neq l \end{cases} \quad (38)$$

Based on (38), it can be obtained that

$$\begin{cases} \mathbf{E}[\tilde{r}_k^2] = 0 \\ \mathbf{E}[\tilde{r}_k^4] = 3\sigma_r^4. \end{cases} \quad (39)$$

The estimation errors contained in $\hat{r}_{3|3}$, $\hat{\eta}_{3|3}$ are expressed as follows:

$$\begin{aligned} \tilde{r}_3 &= \frac{r_3^m - r_2^m}{T} - \frac{r_3 - r_2}{T} = \frac{r_3^m - r_2^m}{T} \\ &\quad - \frac{(r_3^m - \tilde{r}_3) - (r_2^m - \tilde{r}_2)}{T} = \frac{\tilde{r}_3 - \tilde{r}_2}{T}, \end{aligned} \quad (40)$$

$$\begin{aligned} \tilde{\eta}_3 &= \frac{\tilde{r}_2^2 - \tilde{r}_3^2 + \tilde{r}_3 \tilde{r}_2 - \tilde{r}_2 \tilde{r}_1}{T^2} + \\ &\quad \frac{(2r_3^m - r_2^m)\tilde{r}_3 + (r_1^m - 2r_2^m - r_3^m)\tilde{r}_2 + r_2^m \tilde{r}_1}{T^2}. \end{aligned} \quad (41)$$

Based on (38)–(41), the corresponding components of covariance $\mathbf{P}_{3|3}$ in (32) can be calculated as

$$P_{3|3}^{rr} = \sigma_r^2, \quad (42)$$

$$P_{3|3}^{r\dot{r}} = P_{3|3}^{\dot{r}r} = \mathbf{E}[\tilde{r}_3 \tilde{r}_3] = \frac{\sigma_r^2}{T}, \quad (43)$$

$$P_{3|3}^{r\dot{\eta}} = P_{3|3}^{\dot{\eta}r} = \mathbf{E}[\tilde{r}_3 \tilde{\eta}_3] = \frac{(2r_3^m - r_2^m)\sigma_r^2}{T^2}, \quad (44)$$

$$P_{3|3}^{\dot{r}\dot{r}} = \mathbf{E}[\tilde{r}_3^2 \tilde{r}_3] = \frac{2\sigma_r^2}{T^2}, \quad (45)$$

$$P_{3|3}^{r\dot{\eta}\dot{\eta}} = P_{3|3}^{\dot{\eta}\dot{\eta}r} = \mathbf{E}[\tilde{r}_3 \tilde{\eta}_3] = \frac{(3r_3^m + r_2^m - r_1^m)\sigma_r^2}{T^3}, \quad (46)$$

$$\begin{aligned} P_{3|3}^{\dot{\eta}\dot{\eta}} = \mathbf{E}[\tilde{\eta}_3^2 \tilde{\eta}_3] &= \left[\frac{5(r_3^m)^2 + 6(r_2^m)^2}{T^4} + \right. \\ &\quad \left. \frac{(r_1^m)^2 - 2r_3^m r_1^m - 4r_2^m r_1^m}{T^4} \right] \sigma_r^2 + \frac{6\sigma_r^4}{T^4}. \end{aligned} \quad (47)$$

4.2 Model-based initialization

In the TPD-based method, the initialization of the Doppler and converted Doppler components is carried out based on the assumption that the target range varies linearly with time in a sampling interval. However, in reality, this is usually not the case, as presented in (7). When the assumption is violated, the application of the TPD-based method may introduce significant errors into the initial state estimate, resulting in serious performance degradation in the following filtering process. To address this problem, a model-based initialization method is proposed in this paper. The incorporation of the correct information may benefit the estimation accuracy of the new initialization method, especially in scenarios where the nonlinearity with respect to time is strong.

According to (7), ignoring the process noise, the state equation in the R-D plane for the Cartesian CV motion can be written as

$$\begin{bmatrix} r_{k+1} \\ \dot{r}_{k+1} \\ \dot{\eta}_{k+1} \end{bmatrix} = \begin{bmatrix} \sqrt{r_k^2 + 2r_k \dot{r}_k T + \dot{\eta}_k T^2} \\ r_k \dot{r}_k + \dot{\eta}_k T \\ \sqrt{r_k^2 + 2r_k \dot{r}_k T + \dot{\eta}_k T^2} \\ \dot{\eta}_k \end{bmatrix}. \quad (48)$$

It can be obtained that

$$r_{k+1}^2 = r_k^2 + 2r_k \dot{r}_k T + \dot{\eta}_k T^2, \quad (49)$$

$$r_{k+1} \dot{r}_{k+1} = r_k \dot{r}_k + \dot{\eta}_k T. \quad (50)$$

Recursively, the following equation can be obtained:

$$\begin{aligned} r_{k+2}^2 &= r_{k+1}^2 + 2r_{k+1} \dot{r}_{k+1} T + \dot{\eta}_{k+1} T^2 = \\ &r_{k+1}^2 + 2(r_k \dot{r}_k + \dot{\eta}_k T) T + \dot{\eta}_k T^2 = \\ &r_{k+1}^2 + 2r_k \dot{r}_k T + 3\dot{\eta}_k T^2. \end{aligned} \quad (51)$$

Consider $r_k \dot{r}_k$ and $\dot{\eta}_k$ as unknowns, the relationships contained in (49) and (51) can be reformulated in a matrix-form, given by

$$\begin{bmatrix} 2T & T^2 \\ 2T & 3T^2 \end{bmatrix} \begin{bmatrix} r_k \dot{r}_k \\ \dot{\eta}_k \end{bmatrix} = \begin{bmatrix} r_{k+1}^2 - r_k^2 \\ r_{k+2}^2 - r_{k+1}^2 \end{bmatrix}. \quad (52)$$

Solve the above equation, the expressions of $r_k \dot{r}_k$ and $\dot{\eta}_k$ with respect to range components at three consecutive time steps k , $k+1$ and $k+2$ can be obtained as

$$r_k \dot{r}_k = \frac{-r_{k+2}^2 + 4r_{k+1}^2 - 3r_k^2}{4T}, \quad (53)$$

$$\dot{\eta}_k = \frac{r_{k+2}^2 - 2r_{k+1}^2 + r_k^2}{2T^2}. \quad (54)$$

However, in the filter initialization, it is more desired to express the initial state estimate using state components at current or previous time steps rather than the ones at ‘‘future’’ time steps. To this end, according to (48), the recursive relationship between $r_{k+2} \dot{r}_{k+2}$ and $r_k \dot{r}_k$ can be recursively written as

$$r_{k+2} \dot{r}_{k+2} = r_k \dot{r}_k + 2\dot{\eta}_k T. \quad (55)$$

Substitute (53) and (54) into (55):

$$\begin{aligned} r_{k+2} \dot{r}_{k+2} &= \frac{-r_{k+2}^2 + 4r_{k+1}^2 - 3r_k^2}{4T} + \\ &2T \left(\frac{r_{k+2}^2 - 2r_{k+1}^2 + r_k^2}{2T^2} \right) = \frac{3r_{k+2}^2 - 4r_{k+1}^2 + r_k^2}{4T}. \end{aligned} \quad (56)$$

Then, the new formulations can be obtained as

$$\dot{r}_{k+2} = \frac{3r_{k+2}^2 - 4r_{k+1}^2 + r_k^2}{4r_{k+2} T}, \quad (57)$$

$$\dot{\eta}_{k+2} = \dot{\eta}_{k+1} = \dot{\eta}_k = \frac{r_{k+2}^2 - 2r_{k+1}^2 + r_k^2}{2T^2}. \quad (58)$$

For $k=3$, the expression of state using range components at three consecutive time steps is given by

$$\mathbf{x}_3 = \begin{bmatrix} r_3 \\ \dot{r}_3 \\ \dot{\eta}_3 \end{bmatrix} = \mathbf{g}(r_3, r_2, r_1) = \begin{bmatrix} r_3 \\ \frac{3r_3^2 - 4r_2^2 + r_1^2}{4r_3 T} \\ \frac{r_3^2 - r_2^2 + r_1^2}{2T^2} \end{bmatrix}. \quad (59)$$

In tracking applications, the true state of the target is usually not available. Thus, the initial state estimate can

be calculated as the expectation of function $\mathbf{g}(r_3, r_2, r_1)$ conditioning on the range measurements. However, according to (59), r_3 also appears in the denominator of the expression of the Doppler component, which makes the derivation of the conditional mean and corresponding covariance intractable. Here, r_3 , r_2 , and r_1 are replaced by the corresponding measurements to obtain an approximate expression of the initial state estimate as

$$\hat{\mathbf{x}}_{3|3} = \begin{bmatrix} \hat{r}_{3|3} \\ \hat{\dot{r}}_{3|3} \\ \hat{\dot{\eta}}_{3|3} \end{bmatrix} = \mathbf{E}[\mathbf{g}(r_3, r_2, r_1) | r_3^a] \approx \mathbf{g}(r_3^a) = \begin{bmatrix} r_3^m \\ \frac{3(r_3^m)^2 - 4(r_2^m)^2 + (r_1^m)^2}{4r_3^m T} \\ \frac{(r_3^m)^2 - 2(r_2^m)^2 + (r_1^m)^2}{2T^2} \end{bmatrix} \quad (60)$$

where $\mathbf{r}_3^a = [r_3^m, r_2^m, r_1^m]'$ is the stacked vector of range measurements at three consecutive time steps.

Due to the incorporation of the correct dynamic model, the expression of $\hat{r}_{3|3}$ and $\hat{\dot{\eta}}_{3|3}$ in (60) is different from those in (37). It can be seen that r_1^m is involved in the expression of Doppler estimate in (60), which implies that more information is utilized in the initialization process. The UT method [23,24] is adopted to calculate the initial state estimate and the initial covariance matrix according to (60). First, $2n_r + 1$ sigma points and corresponding weights are calculated based on the stacked vector \mathbf{r}_3^a as

$$\left\{ \begin{aligned} \boldsymbol{\gamma}_3^0 &= \mathbf{r}_3^a \\ W^0 &= \frac{\lambda}{n_r + \lambda} \\ \boldsymbol{\gamma}_3^i &= \mathbf{r}_3^a + (\sqrt{(n_r + \lambda) \mathbf{P}_3^r})_i \\ W^i &= \frac{1}{2(n_r + \lambda)} \\ \boldsymbol{\gamma}_3^{i+n_r} &= \mathbf{r}_3^a - (\sqrt{(n_r + \lambda) \mathbf{P}_3^r})_i \\ W^{i+n_r} &= \frac{1}{2(n_r + \lambda)} \end{aligned} \right. \quad (61)$$

where $i = 1, 2, \dots, n_r$, $\mathbf{P}_3^r = \text{diag}\{\sigma_r^2, \sigma_r^2, \sigma_r^2\}$, n_r is the dimension of the stacked vector \mathbf{r}_3^a .

Then, according to (60), the posterior sampling points can be obtained as

$$\hat{\boldsymbol{\gamma}}_{3|3}^i = \mathbf{g}(\boldsymbol{\gamma}_3^i), \quad (62)$$

and the state estimate is given by

$$\hat{\mathbf{x}}_{3|3} = \sum_{i=0}^{2n_r} W^i \hat{\boldsymbol{\gamma}}_{3|3}^i. \quad (63)$$

At last, the initial covariance matrix $\mathbf{P}_{3|3}$ can be calculated as

$$\mathbf{P}_{3|3} = \sum_{i=0}^{2n_r} W^i (\hat{\boldsymbol{\gamma}}_{3|3}^i - \hat{\mathbf{x}}_{3|3})(\hat{\boldsymbol{\gamma}}_{3|3}^i - \hat{\mathbf{x}}_{3|3})'. \quad (64)$$

5. Simulation results

Numerical experiments are performed to examine the effectiveness of the novel approach to estimate range and Doppler of the target using range-only measurements. The proposed methods using the TPD-based and MB initialization methods are compared with two standard Kalman filters with approximate dynamic models in range coordinates: the approximate NCV (ANCV) model and the approximate nearly constant acceleration (ANCA) model [10,38]. Before the accurate dynamic model was established in [21], these models were used to describe the target motion in the R-D plane. That is, the comparison algorithms selected in this paper are classic solutions to the state estimation problem in range coordinate, which are also employed as competitors in [2,21] in cases with measurements of range and Doppler. The state equation of the ANCV model is given as

$$\begin{bmatrix} r_{k+1} \\ \dot{r}_{k+1} \end{bmatrix} = \begin{bmatrix} 1 & T \\ 0 & 1 \end{bmatrix} \begin{bmatrix} r_k \\ \dot{r}_k \end{bmatrix} + \begin{bmatrix} T^2/2 \\ T \end{bmatrix} v_k^r, \quad (65)$$

while the counterpart of the ANCA model is

$$\begin{bmatrix} r_{k+1} \\ \dot{r}_{k+1} \\ \ddot{r}_{k+1} \end{bmatrix} = \begin{bmatrix} 1 & T & T^2/2 \\ 0 & 1 & T \\ 0 & 0 & 1 \end{bmatrix} \begin{bmatrix} r_k \\ \dot{r}_k \\ \ddot{r}_k \end{bmatrix} + \begin{bmatrix} T^2/2 \\ T \\ 1 \end{bmatrix} v_k^r \quad (66)$$

where \ddot{r}_k denotes range acceleration in range coordinate, v_k^r stands for the process noise in range direction, assumed to be zero-mean Gaussian white noise with variance q_r^2 .

The traditional two-point differencing method for one-dimensional models, such as the NCV and NCA models in the x or y axis of Cartesian coordinates, is employed here to initialize the Kalman filters [39]. The formulations are omitted here for brevity. A total of 1 000 Monte Carlo runs are performed over 100 time steps. The PCRLB is calculated to indicate the theoretical benchmark in a given scenario [37]. The normalized estimation error squared (NEES) [39] is adopted to test the consistency of filters.

The target follows the Cartesian NCV motion model. The process noise is with the standard deviation $q = 0.01 \text{ m/s}^2$. The standard deviations of process noises used in the filters with the ANCV or ANCA model are $q_r = 0.1 \text{ m/s}^2$ or $q_r = 0.01 \text{ m/s}^2$, respectively. Note that when the process noises become larger, the approximation error contained in the expression of the process noise in (3) may increase and harm modeling accuracy, leading to performance degradation of the proposed method. This flaw may limit the application of the proposed method in cases with large uncertainty on the prior information of the motion model. A feasible way to mitigate the effect of

the approximation error is to use higher-order approximation techniques in motion modeling. For more detail, please refer to [21].

The location of the sensor is at the origin, reporting range measurements with a sampling interval of $T = 5 \text{ s}$. The standard deviation of range measurement noise is $\sigma_r = 50 \text{ m}$. Two examples with different initial headings of the target are provided to evaluate the performance of the proposed method under conditions with different levels of nonlinearity of the range component.

5.1 Example with the initial heading perpendicular to the radial direction

In this example, the target is first assumed to start from the position of (5 km, 5 km) in the x - y plane of Cartesian coordinates with a high initial speed of 300 m/s and an initial heading of -45° , which is perpendicular to the radial direction. The target trajectory in Cartesian coordinates and the ground truth of the R-D state along with the range measurements are depicted in Fig. 1.

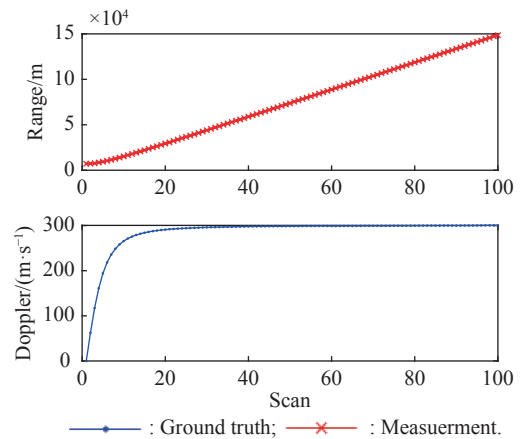
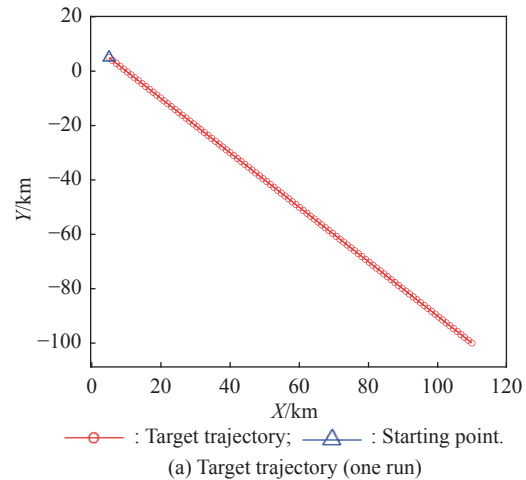
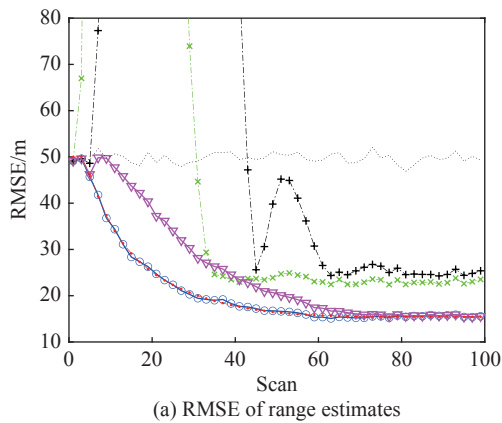
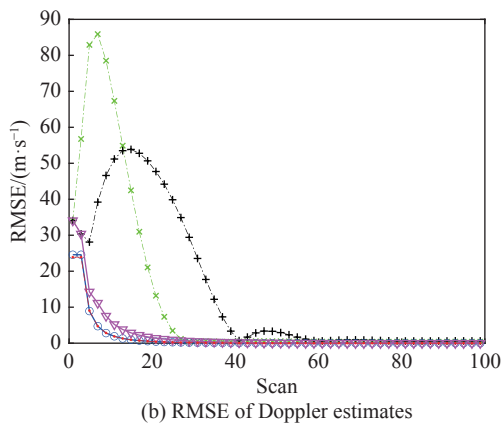


Fig. 1 Ground truth and measurements in the example with the initial heading perpendicular to the radial direction and the initial speed of 300 m/s

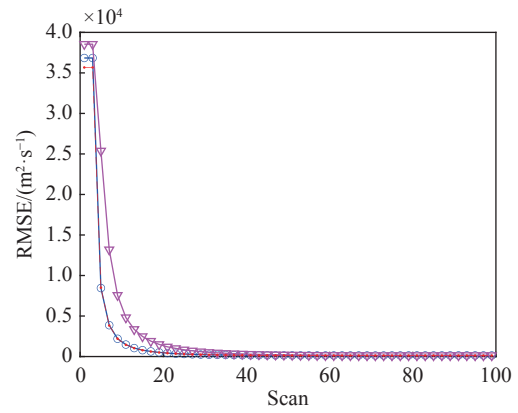
It can be seen that the nonlinearity of the range component with respect to time is pronounced in the first 10 s, thus can be used to show the advantage of the MB initialization method over the TPD-based method. The root mean squared errors (RMSEs) of the filters are shown in Fig. 2(a)–Fig. 2(c). It can be seen that the two proposed methods outperform the two filters with approximate models, which diverge at the early stage of the filtering process. As shown in Fig. 1(b), the nonlinearity of range evolution is strong in the early stage. The ANCV and ANCA models seriously diverge from the true target motion, leading to performance degradation. However, after 40 scans, the evolution of range with respect to time is close to a linear function. The divergence between the approximate models and the true target motion becomes small. Furthermore, as shown in Fig 2(d), the state covariance becomes much larger than the estimation error (NEES is much smaller than 2) in the later stage, which helps the Kalman filter to gradually correct the estimate using measurements over time, resulting in a relatively stable result.



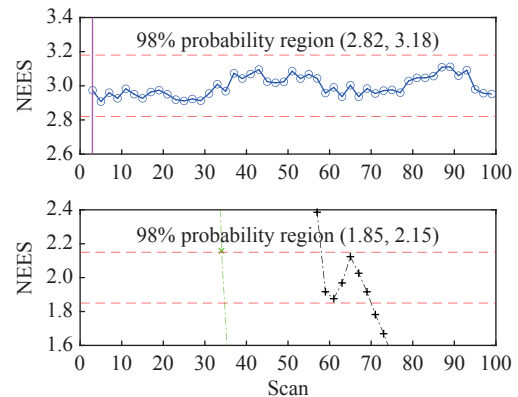
(a) RMSE of range estimates



(b) RMSE of Doppler estimates



(c) RMSE of the third component of state estimates



(d) NEES

—x—: ANCV; —+—: ANCA;
 —○—: Proposed method+MB; —▽—: Proposed method+TPD;
: Measurement; - - - : PCRLB.

Fig. 2 Comparison of filter RMSEs in the example with the initial heading perpendicular to the radial direction and the initial speed of 300 m/s

It can be observed that the RMSE curve of the filter using the ANCA model has two peaks. The first one appears due to the performance degradation arising from mismatch between the ANCA model and the true target motion. The appearance of the second peak is probably because of the effect of the inaccurate estimate of the second-order derivative of range (only included in the ANCA model). As shown in Fig 1(b), the second-order derivative of range decreases from the beginning of the filtering and is close to zero after 50 scans. However, the filter using ANCV assumes a nearly constant acceleration, thus may not be able to capture the change of acceleration timely, resulting in the second RMSE peak around the 50th scan. As shown in Fig. 2(d), in the early stage, the state covariance of the filter using the ANCV model is much smaller than the estimation error (NEES is much larger than 2), which means the filter is “optimistic”. That is, the filter overly trusts the dynamic model rather than the measurements in the update of state estimates. As shown in Fig 1, in the very beginning, the divergence

between the true target motion and the ANCA model is slight. Thus, the RMSE first decreases. As the divergence becomes pronounced, the RMSE turns to increase.

Among the two proposed methods, the one using the MB initialization method shows better performance and meets well with the PCRLB during the whole filtering process. The RMSE of the TPD-based method increases first because it suffers from a model mismatch while the model-based method incorporates the correct information of the dynamic model. However, the model mismatch only exists in the filtering initialization. In the filtering procedure, the state estimate and estimate covariance are continuously updated using the accurate dynamic model and range measurements over time. During the process, the effect of the mismatch will be gradually reduced. Thus, the RMSE stops increasing at some point and starts to decrease. With enough time, the proposed method using the TPD initialization method finally converges and achieves comparable performance with the one using the MB method.

Fig. 1(d) depicts the NEES values of the filters along with the 98 % probability regions. It can be seen that only the state estimates produced by the proposed method using the MB initialization method are consistent in all scans. Both the RMSE and NEES results illustrate the validity and correctness of the proposed method.

Then, the simulation is carried out in another case where the initial speed of the target is reduced to 20 m/s without changing other parameters. The target trajectory, ground truth, and range measurements are depicted in Fig. 3. It can be observed that the nonlinearity of range with respect to time becomes weak. The RMSEs of the filters are shown in Fig. 4(a)–Fig. 4(c). It can be seen that the two proposed methods using different initialization methods have almost the same level of RMSE close to the PCRLB, except for the initial phase, where the MB method yields larger estimation errors compared with the TPD-based method. This is because when the nonlinearity of range is weak, the effect of the model mismatch in the TPD-based method on the performance is mitigated. While the strong nonlinearity in the formulation of the Doppler component in (56) has a detrimental impact on the estimation accuracy of the MB method, resulting in a higher level of RMSE compared with the TPD-based method. On the contrary, the performance of the methods using the ANCV and ANCA models starts to degrade after 20–30 scans since they fail to correctly describe the Cartesian NCV motion in range coordinate. It can also be seen that in the first 20 scans, the RMSEs of the filter using the ANCV model are lower than those of the proposed method. However, according to the consistency testing results shown in Fig. 2(d), the filters using the

ANCV and ANCA models are inconsistent. Fig. 2(d) also shows that both the two proposed methods produce consistent state estimates.

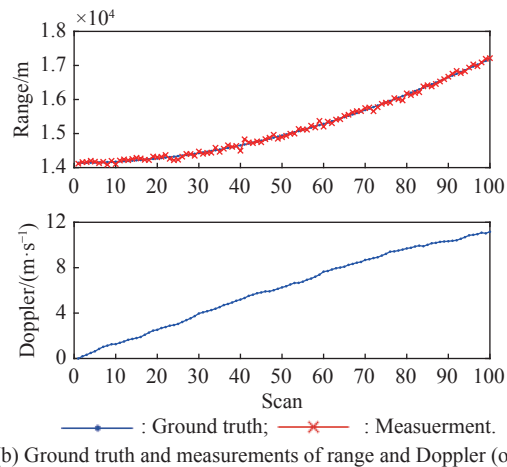
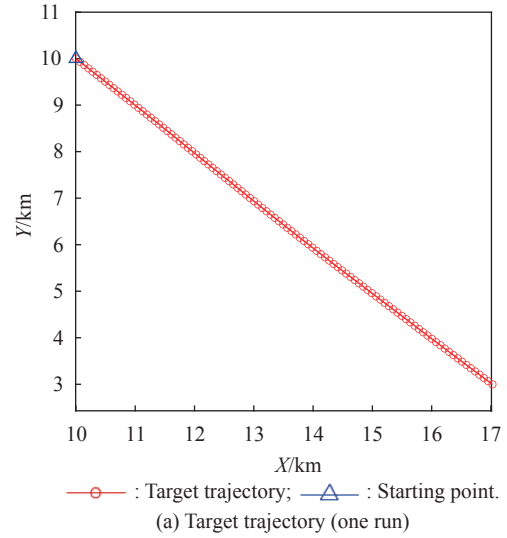
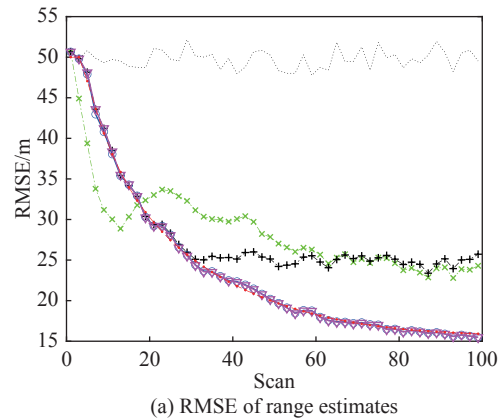


Fig. 3 Ground truth and measurements in the example with the initial heading perpendicular to the radial direction and the initial speed of 20 m/s



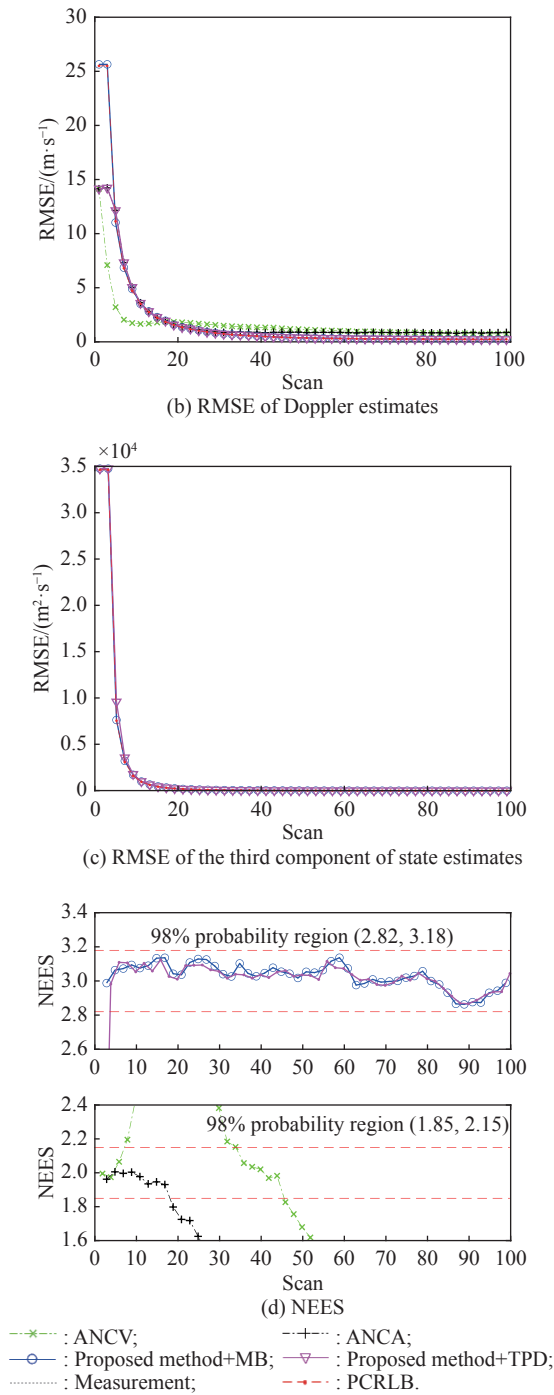


Fig. 4 Comparison of filter RMSEs in the example with the initial heading perpendicular to the radial direction and the initial speed of 20 m/s

5.2 Example with the initial heading in the radial direction

The initial heading of the target is changed to 45°, which is away from the sensor, to examine the performance of the proposed method when the nonlinearity of the range component with respect to time is weak. The other

parameters remain the same as the previous example.

First, the target is assumed to have a high initial speed of 300 m/s. The target trajectory, ground truth, and range measurements are depicted in Fig. 5. The RMSEs of the filters are shown in Fig. 6(a)–Fig. 6(c). It can be seen that the RMSEs at the steady state can be sorted into two groups with a descending order of magnitude: the filters using the ANCV model and the ANCA model, the two proposed filters. The two proposed filters outperform the filters using the approximate dynamic models because of the incorporation of correct model information. Although different initialization methods are employed in the two proposed filters, they produce state estimates with almost the same level of RMSE that is close to the PCRLB, which demonstrates the effectiveness of the two initialization methods. The filter using the ANCV model converges the most quickly. However, this filter along with the one using the ANCA model is demonstrated to be inconsistent by the NEES results shown in Fig. 6(d). It is also shown in Fig. 6(d) that the two proposed filters are consistent in all scans.

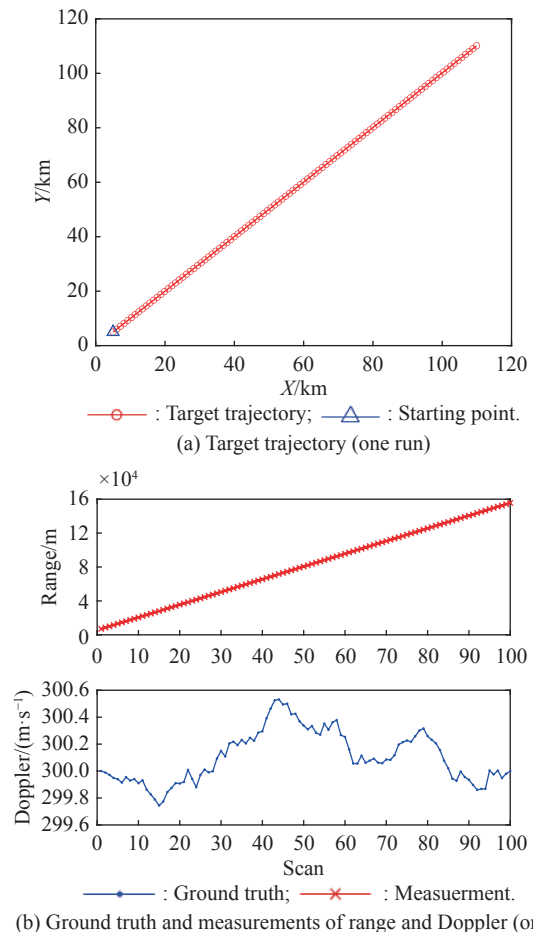
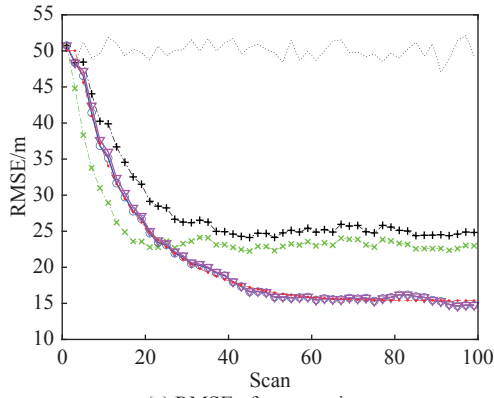
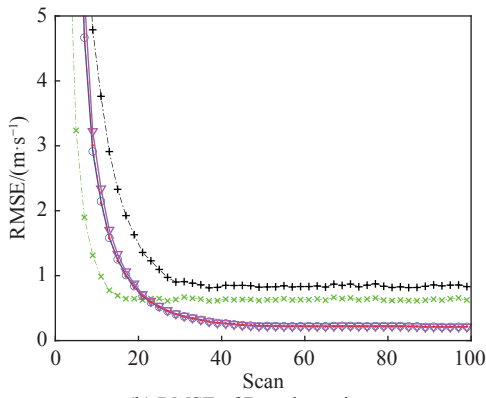


Fig. 5 Ground truth and measurements in the example with the initial heading in the radial direction and the initial speed of 300 m/s

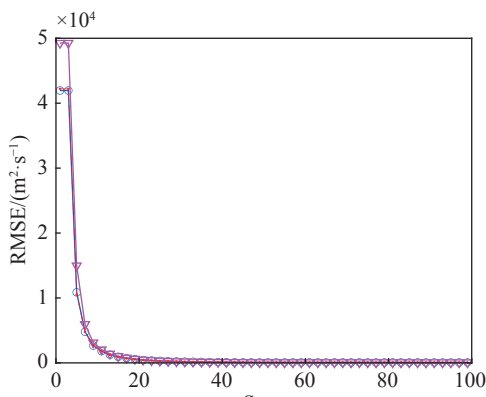
In the following simulation, a much lower initial speed of 20 m/s is assumed for the target, which means the true dynamic model of the target is closer to a linear one, as shown in Fig. 7. The RMSE and NEES results shown in Fig. 8 are similar to those displayed in Fig. 8, which again illustrates the effectiveness of the proposed method.



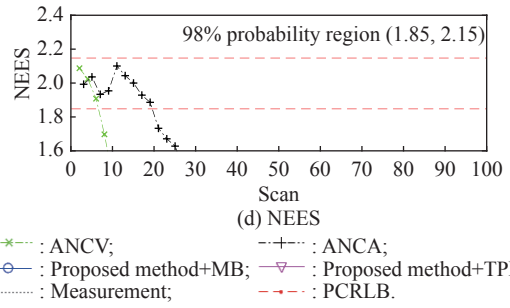
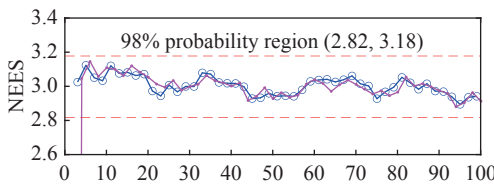
(a) RMSE of range estimates



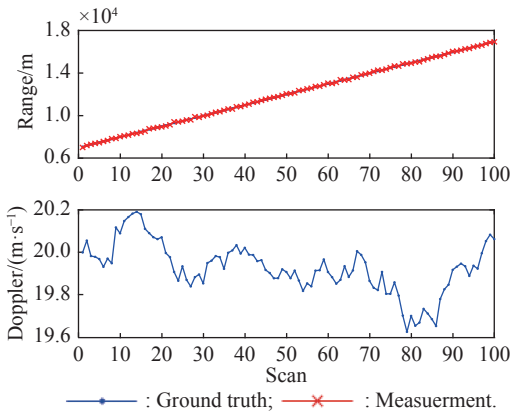
(b) RMSE of Doppler estimates



(c) RMSE of the third component of state estimates



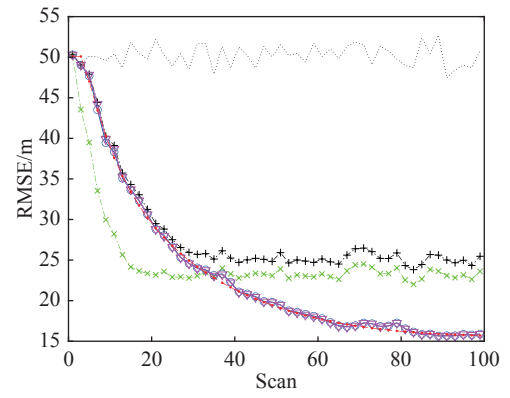
(a) Target trajectory (one run)



(b) Ground truth and measurements of range and Doppler (one run)

Fig. 6 Comparison of filter RMSEs in the example with the initial

Fig. 7 Ground truth and measurements in the example with the initial heading in the radial direction and the initial speed of 20 m/s



(a) RMSE of range estimates

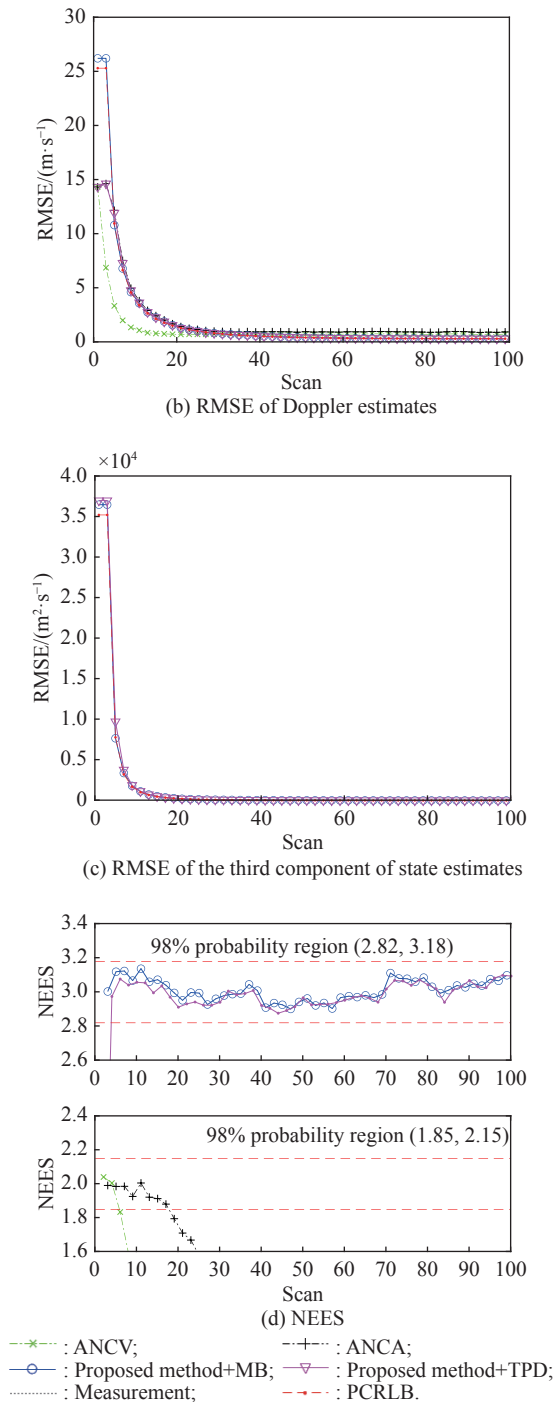


Fig. 8 Comparison of filter RMSEs in the example with the initial heading in the radial direction and the initial speed of 20 m/s

heading in the radial direction and the initial speed of 300 m/s

6. Conclusions

The state estimation problem in range coordinate using range-only measurements has been investigated in this paper. A state estimation method, which is implemented based on the corresponding state equation in the R-D

plane for the Cartesian NCV motion and the measurement equation with range-only measurements, is proposed. The UKF is employed to address the nonlinearity contained in the dynamic model. Two filtering initialization methods are developed. One is derived in an analytical form based on the two-point differencing approach. While the other uses the UT method to calculate the initial state estimate and covariance from range measurements according to the nonlinear formulation derived using the correct dynamic information, resulting in a model-based method. Due to the incorporation of correct model information, the MB method exhibits superior performance compared with the TPD-based method, especially in the case when nonlinearity of the range component with respect to time is pronounced. The effectiveness and superior performance of the proposed estimation and initialization methods are demonstrated through numerical experiments in two examples.

In future works, it is of interest to extend the proposed state estimation method to cases with more complex motions of the target, such as maneuvering target tracking problems. Furthermore, how to integrate the proposed method into the framework of multiple target tracking deserves investigation.

References

- [1] BRANKOR, SANJEEV A, JAMES M. Target motion analysis using range-only measurements: algorithms, performance and application to ISAR data. *Signal Processing*, 2002, 82(2): 273–296.
- [2] ZHOU G J, ZHOU J F, FU T J, et al. Multisensor-multitarget tracking based on hierarchical association only using range-Doppler measurements. *Proc. of the IET International Radar Conference*, 2013: 327–340.
- [3] TOBIAS M, LANTERMAN A D. A probability hypothesis density-based multitarget tracker using multiple bistatic range and velocity measurements. *Proc. of the 36th Southeastern Symposium on System Theory*, 2004: 205–209.
- [4] JAUFFRET C, PEREZ A, PILLON D. Observability: range-only versus bearings-only target motion analysis when the observer maneuvers smoothly. *IEEE Trans. on Aerospace and Electronic Systems*, 2017, 53(6): 2814–2832.
- [5] PILLON D, PEREZ-PIGNOL A, JAUFFRET C. Observability: range-only vs. bearings-only target motion analysis for a leg-by-leg observers trajectory. *IEEE Trans. on Aerospace and Electronic Systems*, 2016, 52(4): 1667–1678.
- [6] SONG T L. Observability of target tracking with range-only measurements. *IEEE Journal of Oceanic Engineering*, 1999, 24(3): 383–387.
- [7] COLEMAN D, BOPARDIKAR S D, TAN X. Observability-aware target tracking with range only measurement. *Proc. of the American Control Conference*, 2021: 1–8.
- [8] CLARK J M, KOUNTOURIOTIS P A, VINTER R B. A Gaussian mixture filter for range-only tracking. *IEEE Trans. on Automatic Control*, 2011, 56(3): 602–613.
- [9] MANOLAKIS D E. Efficient solution and performance analysis of 3-D position estimation by trilateration. *IEEE Trans. on Aerospace and Electronic Systems*, 1996, 32(4):

- 1239–1248.
- [10] DEMING R, SCHINDLER J, PERLOVSKY L. Multi-target/multi-sensor tracking using only range and Doppler measurements. *IEEE Trans. on Aerospace and Electronic Systems*, 2009, 45(2): 593–611.
- [11] MASHHADANI W A, DANOON L, BROWN A. Modeling range-only multistatic radar target detection with interval analysis in 3D. *Proc. of the European Radar Conference*, 2016: 173–176.
- [12] PETSIOS M N, ALIVIZATOS E G, UZUNOGLU N K. Manoeuvring target tracking using multiple bistatic range and range-rate measurements. *Signal Processing*, 2007, 87(4): 665–686.
- [13] YANG X S, ZHANG W A, LIU A D, et al. Linear fusion estimation for range-only target tracking with nonlinear transformation. *IEEE Trans. on Industrial Informatics*, 2020, 16(10): 6403–6412.
- [14] ZHAO Y S, HU D X, ZHAO Y J, et al. Moving target localization for multistatic passive radar using delay, Doppler and Doppler rate measurements. *Journal of Systems Engineering and Electronics*, 2020, 31(5): 939–949.
- [15] PACHOLSKA M, DUMBGEN F, SCHOLEFIELD A. Relax and recover: guaranteed range-only continuous localization. *IEEE Robotics and Automation Letter*, 2020, 5(2): 2248–2255.
- [16] SADEGHI M, BEHNIA F, AMIRI R. Optimal sensor placement for 2-D range-only target localization in constrained sensor geometry. *IEEE Trans. on Signal Processing*, 2020, 68: 2316–2327.
- [17] DASH D, JAYARAMAN V. A probabilistic model for sensor fusion using range-only measurements in multistatic radar. *IEEE Sensors Letter*, 2020, 4(6): 7500604.
- [18] MA H, ANTONIOU M, STOVE A G, et al. Target kinematic state estimation with passive multistatic radar. *IEEE Trans. on Aerospace and Electronic Systems*, 2021, 57(4): 2121–2134.
- [19] BARRICK D. History, present status, and future directions of HF surface-wave radars in the U. S. *Proc. of the International Conference on Radar*, 2003: 652–655.
- [20] GRIFFITHS H. Multistatic, MIMO and networked radar: the future of radar sensors. *Proc. of the 7th European Radar Conference*, 2010: 81–84.
- [21] ZHOU G J, GUO Z K, LI K Y, et al. Motion modeling and state estimation in range-Doppler plane. *Aerospace Science and Technology*, 2021, 115: 106792.
- [22] LI K Y, GUO Z K, ZHOU G J. Nearly constant acceleration model for state estimation in the range-Doppler plane. *IET Radar, Sonar & Navigation*, 2021, 15(12): 1687–1701.
- [23] JULIER S J, UHLMANN J K, DURRANT-WHYTE H F. A new method for nonlinear transformation of means and covariances in filters and estimates. *IEEE Trans. on Automatic Control*, 2000, 45(3): 477–482.
- [24] JULIER S J, UHLMANN J K. Unscented filtering and nonlinear estimation. *Proceedings of the IEEE*, 2004, 92(3): 401–422.
- [25] WAN E A, VAN D M R. The unscented Kalman filter for nonlinear estimation. *Proc. of IEEE Symposium on Adaptive Systems for Signal Processing, Communication and Control*, 2000: 153–158.
- [26] LIU C Y, SHUI P L, WEI G, et al. Modified unscented Kalman filter using modified filter gain and variance scale factor for highly maneuvering target tracking. *Journal of Systems Engineering and Electronics*, 2014, 25(3): 380–385.
- [27] DENG F, CHEN J, CHEN C. Adaptive unscented Kalman filter for parameter and state estimation of nonlinear high-speed objects. *Journal of Systems Engineering and Electronics*, 2013, 24(4): 655–665.
- [28] GUO Z K, ZHOU G J. State estimation from range-only measurements. *Proc. of the 23rd International Conference on Information Fusion*, 2020: 367–372.
- [29] ZHOU G J, PELLETIER M G, KIRUBARAJAN T, et al. Statically fused converted position and Doppler measurement Kalman filters. *IEEE Trans. on Aerospace and Electronic Systems*, 2014, 50(1): 300–318.
- [30] ZHOU G J, WU L G, XIE J H, et al. Constant turn model for statically fused converted measurement Kalman filters. *Signal Processing*, 2015, 108: 400–411.
- [31] ARASARATNAM I, HAYKIN S. Cubature Kalman filter. *IEEE Trans. on Automatic Control*, 2009, 54(6): 1254–1269.
- [32] SHI J, QI G Q, LI Y Y, et al. Stochastic convergence analysis of cubature Kalman filter with intermittent observations. *Journal of Systems Engineering and Electronics*, 2018, 29(4): 823–833.
- [33] ARULAMPALAM M S, MASKELL S, GORDON N, et al. A tutorial on particle filters for online nonlinear/non-Gaussian Bayesian tracking. *IEEE Trans. on Signal Processing*, 2002, 50(2): 174–188.
- [34] DAN C, DOUCET A. A survey of convergence results on particle filtering methods for practitioners. *IEEE Trans. on Signal Processing*, 2002, 50(3): 736–746.
- [35] ZHANG Y, WANG S F, LI J C. Improved particle filtering techniques based on generalized interactive genetic algorithm. *Journal of Systems Engineering and Electronics*, 2016, 27(1): 242–250.
- [36] ZUO J Y, ZHONG X P. Particle filter for nonlinear systems with multi-sensor asynchronous random delays. *Journal of Systems Engineering and Electronics*, 2017, 28(6): 1064–1071.
- [37] TICHAVSKY P, MURAVCHIK C H, NEHORAI A. Posterior Cramer-Rao bounds for discrete-time nonlinear filter. *IEEE Trans. on Signal Processing*, 1998, 46(5): 1386–1396.
- [38] LI X R, JILKOV V P. Survey of maneuvering target tracking. Part I: dynamic models. *IEEE Trans. on Aerospace and Electronic Systems*, 2003, 39(4): 1333–1364.
- [39] BAR-SHALOM Y, LI X R, KIRUBARAJAN T. Estimation with applications to tracking and navigation: theory, algorithms, and software. New York: Wiley, 2001.

Biographies



LI Keyi was born in 1991. He received his B.E. degree in communication engineering and M.E. and Ph.D. degrees in information and communication engineering from Harbin Institute of Technology, Harbin, China, in 2014, 2016, and 2020, respectively. He is currently a lecturer in the School of Electronics and Information Engineering, Harbin Institute of Technology, Harbin, China. From November 2020, he held a Postdoctoral Fellowship in the Department of Aerospace Engineering, Harbin Institute of Technology. From September 2018 to September 2019, supported by China Scholarship Council, he was a visiting Ph.D. student in McMaster University, Hamilton, ON, Canada. His research interests include estimation, target tracking and information fusion.

E-mail: likeyi@hit.edu.cn



GUO Zhengkun was born in 1985. He received his B.E. degree from the School of Electronic Information, Wuhan University, Wuhan, China, in 2008, his M.E. degree from Shanghai Academy of Spaceflight Technology, Shanghai, China, in 2011 and his Ph.D. degree from the School of Electronics and Information Engineering, Harbin Institute of Technology, Harbin, China. He is currently

working as an assistant engineer in Shanghai Academy of Spaceflight Technology. From March 2016 to March 2017, supported by China Scholarship Council, he was a visiting Ph.D. student in McMaster University, Hamilton, ON, Canada. His research interests include signal processing, estimation, tracking and information fusion.

E-mail: guozkbetter@163.com



ZHOU Gongjian was born in 1979. He received his B.E., M.E., and Ph.D. degrees in information and communication engineering from Harbin Institute of Technology, Harbin, China, in 2000, 2002, and 2008, respectively. From February 2009 to March 2011, he held a Postdoctoral Fellowship in the Department of Aerospace Engineering, Harbin Institute of Technology. From

April 2011 to May 2012, he was a visiting professor with the Department of Electrical and Computer Engineering, McMaster University, Hamilton, ON, Canada. He is currently a professor with the Department of Electronic Engineering, Harbin Institute of Technology. He is also a Longjiang Young Scholar. His research interests include estimation, tracking, detection, information fusion and signal processing.

E-mail: zhougj@hit.edu.cn